



ELSEVIER

Journal of Chromatography A, 969 (2002) 229–243

JOURNAL OF  
CHROMATOGRAPHY A

www.elsevier.com/locate/chroma

# Surface and thermodynamic characterization of conducting polymers by inverse gas chromatography I. Polyaniline

Ali Al-Ghamdi<sup>1</sup>, Zeki Y. Al-Saigh\*

*Department of Chemistry, Buffalo State, State University of New York, 1300 Elmwood Avenue, Buffalo, NY, USA*

## Abstract

The surface thermodynamic characteristics of both doped polyaniline (PANI-HEBSA) and the non-conducting form (PANI-EB) were investigated using inverse gas chromatography. Fourteen solutes were injected into two separate chromatographic columns containing PANI-EB and PANI-HEBSA. All solutes interacted strongly with the conducting form PANI-HEBSA; in particular, undecane and dodecane showed stronger interaction due to the increase of the dispersive forces. Methanol and ethanol showed stronger H-bonding with the conducting form than propanol and butanol. A curvature was observed for acetates and alcohols with a maximum of around 145 °C as an indication of a phase change from a semicrystalline to amorphous phase.  $\Delta H_1^s$  value increased considerably (–3.35 to –46.44 kJ/mol) while the  $\Delta H_1^s$  for the undoped PANI (PANI-EB) averaged about –0.03 kJ/mol. PANI-EB–alkane interaction parameters were measured and ranged from +0.40 to +1.50 (endothermic). However, PANI-HEBSA showed an exothermic behavior due to the polar surface (–1.50 to +1.2). Interaction parameters decreased as the temperature increased and are characteristic of the strong interaction. The dispersive surface energy of the non conducting PANI-EB ranged from 29.13 mJ/m<sup>2</sup> at 140 °C to 94.05 mJ/m<sup>2</sup> at 170 °C, while the surface energy of the conducting PANI-HEBSA showed higher values (150.24 mJ/m<sup>2</sup> at 80 °C to 74.27 mJ/m<sup>2</sup> at 130 °C).  $\gamma_s^d$  values for PANI-EB were found to be higher than expected. The trend of the  $\gamma_s^d$  change direction is also surprising and unexpected due to the thermal activation of the surface of the polymer and perhaps created some nano-pores resulting in an increase in surface energy of the non-conducting form.

© 2002 Published by Elsevier Science B.V.

*Keywords:* Thermodynamic parameters; Inverse gas chromatography; Surface characteristics; Polymers; Polyaniline

## 1. Introduction

Although polyaniline (PANI) has been known for over 100 years, it was only recently found to exhibit unusual chemical, electrical, and optical phenomena, both in insulating and conducting forms. These

unique properties make PANI useful in many applications, particularly in energy storage, electronics, photovoltaic devices, displays, and sensors. The unique properties have led to an interest in the potential use of PANI as a new class of conductors. This interest was generated due to the relative ease of synthesis, low cost, and the stability of PANI in air. However, the insulating form of PANI, polyaniline emeraldine base (PANI-EB), suffers from limited solubility in organic solvents. This difficulty was recently resolved by Cao et al. [1] by func-

\*Corresponding author. Fax: +1-253-679-5907.

E-mail address: [alsaighz@buffalostate.edu](mailto:alsaighz@buffalostate.edu) (Z.Y. Al-Saigh).

<sup>1</sup>Present address: King Abdulaziz Military Academy, P.O. Box 73040, Riyadh 11538, Saudi Arabia.

tionalizing the dopant counter-anion with polar and non-polar analogs to increase solubility in organic solvents.

Recently, inverse gas chromatography (IGC) has emerged as a promising method for polymers and polymer blend characterization [2]. It was shown that the IGC method can be useful in obtaining thermodynamic data on polymeric systems even when the morphology is complex [3]. IGC is often called the molecular probe technique. The term inverse refers to the polymer that can be studied in the solid-phase as the stationary phase, unlike conventional GC where the separation of solvents (solute) is the prime interest. PANI has a limited solubility in solvents; however, IGC is a method of choice for the characterization of PANI because all small organic molecules will have measurable solubilities in solid organic polymers. Hence the range of interactions which can be probed by the IGC technique is unlimited. IGC has been shown to be valuable for the identification of several types of interaction in molecular and macromolecular systems and for the characterization of the bulk and surface of finely divided materials. IGC has been also recognized for the study of the surface energetics of several systems and their response to actual conditions [4]. The attraction of the IGC method lies in its ability to generate fast and accurate physicochemical data on polymeric systems. It is a relatively rapid, convenient method and has the flexibility of selecting the desired temperature ranges.

Although IGC was successfully applied for the determination of the surface energy of several polymeric systems and fillers [5–21], only a few applications of IGC to conducting polymers were reported [22–24]. Conducting and insulating forms of polypyrrole and chemically synthesized polypyrrole doped by chloride (PPyCl) and its related dedoped form (PPyD) have received much of the attention using IGC [22–24]. The effect of dopant on the dispersive and specific properties, and the Lewis acid–base properties of polypyrrole were investigated [22–24]. Most IGC studies were directed to the composition, conductivity, and adhesion properties of these materials.

In our laboratory, we are interested in the determination of the surface thermodynamic characteristics of both doped (PANI-HEBSA) and the non-

conducting form (PANI-EB). Our goal is to apply the IGC method to several systems containing conducting and insulating forms of polyaniline. In this study, we aim to test the IGC method on complex systems and to obtain physicochemical properties on the bulk and on the surface of these materials. In this paper, we report the first series of the characterization of the conducting and the insulating form of polyaniline.

Polyaniline has not yet been characterized using the IGC method owing to the difficulty of the solubility of PANI-EB and the preparation of a chromatographic column containing PANI-EB as a stationary phase. However, there is only one report regarding the surface energy of the conducting form of PANI [24]. The surface energy of the conductive form of PANI was determined as 89.00 mJ/m<sup>2</sup> by IGC which indicates that PANI can be classified as a high energy material.

## 2. Data reduction

### 2.1. Thermodynamics of IGC

A complete analysis of the thermodynamics of IGC was recently reviewed [2]. Thermodynamic quantities can be easily obtained from the chromatographic quantities in IGC by measuring the specific retention volume  $V_g^o$ .  $V_g^o$  is commonly used to describe the elution behavior of solutes and it is defined as:

$$V_g^o = \Delta t \cdot \frac{F}{w} \cdot \frac{273.15}{T_r} \cdot \frac{3}{2} \cdot \frac{\left(\frac{P_i}{P_o}\right)^2 - 1}{\left(\frac{P_i}{P_o}\right)^3 - 1} \quad (1)$$

Here,  $\Delta t = t_s - t_m$  is the difference between the retention time of the solute  $t_s$  and of an unretained solute (marker)  $t_m$ .  $F$  is the flow-rate of the carrier gas measured at room temperature  $T_r$ ,  $w$  is the mass of the stationary phase, and  $P_i$  and  $P_o$  are the inlet and outlet pressures, respectively, and are used for the correction for the compressibility of the carrier gas.

When a polymer is coated onto the solid support, the interaction parameters of the solute–polymer can

then be calculated using  $V_g^o$  measured according to Eq. (1), as follows:

$$\chi_{12} = \ln \frac{273.15R\nu_2}{V_g^o V_1 P_1^o} - 1 + \frac{V_1}{M_2 \nu_2} - \frac{B_{11} - V_1}{RT} \cdot P_1^o \quad (2)$$

Eq. (2) is used routinely for calculation of  $\chi_{12}$  from IGC experiments. Where  $\chi_{12}$  is the polymer–solute interaction parameter, 1 denotes the solute and 2 denotes the polymer,  $\nu_2$  is the specific volume of the polymer at column temperature  $T$ ,  $M_1$  is the molecular mass of the solute,  $V_1$  is the molar volume of the solute,  $R$  is the gas constant, and  $B_{11}$  is the second virial coefficient of the solute in the gaseous state.

Utilizing  $V_g^o$  from the chromatographic quantities, the molar heat and free energy of adsorption can be calculated as in Eq. (3):

$$\Delta H_1^s = -R \cdot \frac{\delta(\ln V_g^o)}{\delta(1/T)} \quad (3)$$

$$\Delta G_1^s = -RT \ln \left( \frac{M_1 V_g^o}{273.15R} \right) \quad (4)$$

## 2.2. Surface energy of polymers

Recently, a complete theoretical treatment for the calculation of the dispersive component of the surface energy of polymers using alkanes was published elsewhere [2,4]. The surface energy,  $\gamma_s$ , can be obtained from the IGC experiments. The surface energy describes interactions due to dispersive forces or a combination of dispersive forces with H-bonding or with dipole–dipole forces. Fowkes [25,26] first reported this method of characterization.

From gas chromatographic measurements,  $V_g^o$  can be related to  $\Delta G_1^s$  (Eq. (4)) as follows:

$$\Delta G_1^s = -RT \ln V_g^o + C \quad (5)$$

Family plots of  $RT \ln V_g^o$  versus the number of carbons in the alkane family should yield the molar free energy of adsorption;  $\Delta G_1^s$ .  $C$  is a constant depending on  $A$ . Eq. (5) relates the energy of adsorption to the surface energy as follows:

$$RT \ln V_g^o + C = 2Na \sqrt{\gamma_s^d \gamma_i^d} \quad (6)$$

$\gamma_s^d$  and  $\gamma_i^d$  are the dispersive components of the solid surface and the interactive solutes phase, respectively.  $N$  is Avogadro's number and  $a$  is the area of the

adsorbed molecules (solutes). In IGC experiments, a series of interactive solutes, such as alkanes, can be injected into the chromatographic column in order to determine the dispersive surface energy,  $\gamma_s^d$ .

Eq. (6) can be rewritten to yield the dispersive surface energy as follows:

$$\gamma_s^d = \frac{1}{4\gamma_{CH_2}} \left[ \frac{\Delta G_a^{CH_2}}{N a_{CH_2}} \right]^2 \quad (7)$$

where  $\gamma_{CH_2}$  is the surface energy of a hydrocarbon consisting only of  $n$ -alkanes,  $a_{CH_2}$  is the area of one  $-CH_2-$  group. Eq. (7) usually tests the IGC method for obtaining the dispersive surface energy of polymers.

## 3. Experimental

### 3.1. Materials

PANI-EB is the non-conducting form and it is a difficult material to process; it has very low solubility in common solvents. PANI-EB was obtained from General Motors Polymer Research Labs with a molecular mass of 55,000 as determined by gel permeation chromatography (GPC) and specific volume of 0.6585 ml/g.

PANI-HEBSA, in the conducting form, was obtained also from General Motors Polymer Research Labs with a molecular mass of 55,000 as determined by GPC. A 2.15% (w/w) of polyaniline salt fully doped with ethylbenzene sulfonic acid was dissolved in hexafluoroisopropanol (HFIP) to form a solution. In order to prepare a chromatographic column according to the method reported earlier [3], 0.2270 g of PANI-EB and 0.298 g of PANI-HEBSA were dissolved in 25 ml (HFIP) and coated onto a chromatographic support separately. HFIP was obtained from Alfa products (Johnson Matthey).

Three chemically different families of solutes were used in this work. Vanishingly small amounts of a series of alkanes, acetates, and alcohols were injected into the chromatographic column. These solutes will probe the dispersive, dipole, and hydrogen bonding interactions with the PANI-EB and PANI-HEBSA backbones. A total of 14 solutes, chromatographic grade, were purchased from Aldrich. Their purity

was checked by gas chromatography prior to use. Chromatographic support, Chromosorb W AW-DMCS (60–80 mesh), was obtained from Analabs. Chromatographic columns were made in the laboratory from 5 ft  $\times$  1/4 in O.D. copper tubing (1 ft = 30.48 cm; 1 in = 2.54 cm) which was purchased locally. All copper columns were washed with methanol and annealed for several hours before use. The resulting load of the PANI-EB and PANI-HEBSA on the column was about 7%. The coating and the annealing processes as well as the chemical composition of both the chromatographic support and PANI were checked by X-ray photon spectroscopy (XPS) experiments as follows.

A VG ESCALAB MK1 spectrometer (based at ITODYS, Université Paris 7, Denis Diderot, Paris, France) equipped with a twin anode was used. Polychromatic Al K $\alpha$  X-ray source (1486.6 eV) has been selected and operated at a power of 200 W (10 kV with an emission current of 20 mA). The pass energy was set at 50 eV. The pressure in the analysis chamber was ca.  $1 \times 10^{-9}$  mbar. The data were collected with Pisces software (Dayta Systems, Bristol, UK). The step size was 1 and 0.1 eV for the survey and the narrow scans, respectively.

Data processing was achieved with Winspec software, kindly supplied by the Laboratoire Interdisciplinaire de Spectroscopie Electronique (LISE, Namur, Belgium). The spectra were corrected for static charging by setting the C1s peak maximum at 285 eV. The surface composition was determined using experimental sensitivity factors. The fractional concentration of a particular element A (%A) was computed using:

$$\%A = \frac{(I_A/s_A)}{\sum(I_n/s_n)} \cdot 100 \quad (8)$$

where  $I_n$  and  $s_n$  are the integrated peak areas and the sensitivity factors, respectively.

### 3.2. Instrumentation and procedure

Chromatographic measurements were made using a modified conventional Hewlett-Packard 5730A gas chromatograph equipped with a thermal conductivity detector. The chromatograph was modified to allow continuous monitoring of the carrier gas flow-rate,

the inlet and outlet pressure, and the column temperature. These modifications along with the complete chromatographic procedure were reported in our earlier publications [3]. Continuous monitoring is important because it reduces experimental error significantly in the four measurable parameters mentioned in Eq. (1). This procedure yielded better-controlled, measurable quantities. The monitored parameters are usually measured over a period of 7 h and then their values are averaged. To avoid change in the morphology of PANI-EB and PANI-HEBSA such as recrystallization, the chromatograph was kept operational at all times. During the course of the experiments, the oven temperature was uniformly increased until a complete set of data was obtained. Control of the mass of both polymers in the stationary phase has been modified and a new method for coating the polymer was developed and recently reported [27]. Solutions of PANI-EB and PANI-HEBSA were dissolved in 25 ml of hexafluoroisopropanol to form solutions of 0.567% (w/w). These solutions were deposited on 7.9 g of a solid support (Chromosorb W) using our soaking method mentioned earlier. A flow-rate of 8 ml/min was used throughout this work in order to eliminate the kinetic effect of flow-rate on  $V_g^o$  values. Flow rates above 10 ml/min may cause a considerable error in the retention volumes, particularly if helium is used as a carrier gas [28].

Retention time of solutes was measured on a completely automated data handling system. An analog/digital data acquisition board (IEEE-488) in the form of a Keithly digital multimeter was interfaced with a personal computer containing a second IEEE-488 board. This allowed for precise measurements of the retention times of the solutes injected into the chromatographic column. The chromatographic signal was analyzed as a function of time and the data from each injection were stored in a separate file for further thermodynamic calculations. This automated system was fast and ideal for routine IGC measurements.

### 3.3. Chemicals and equipment

Polyaniline was purchased from Aldrich (Milwaukee, WI, USA). Fourteen solutes, pentane, hexane, heptane, octane, nonane, decane, undecane, and

dodecane were also purchased from Aldrich. Ethylbenzene sulfonic acid was also purchased from Aldrich. Hexafluoroisopropanol was purchased from Alfa Products, Johnson Matthey (Danvers, MA, USA). Chromasorb W was purchased from Analabs (North Haven, CT, USA). The HP 5730A gas chromatograph was purchased from Hewlett-Packard (Palo Alto, CA, USA). The vacuum generator (VG ESCALAB MK1) spectrometer was manufactured in East Grinstead, UK. Winspec software was kindly supplied by the Laboratoire Interdisciplinaire de Spectroscopie Electronique (LISE, Namur, Belgium). Copper tubing was purchased from the local market. A Keithly digital multimeter equipped with IEEE-488 was purchased from Keithly Electronics (Cleveland, OH, USA).

## 4. Results and discussion

### 4.1. Surface analysis using XPS

Fig. 1 displays the survey scans of Chromosorb W and PANI coated on Chromosorb W after a heat treatment. There is a significant increase in the C1s peak intensity when PANI is coated on the support; however, the N1s is not straightforwardly detected on the wide scan. N1s peak is only visible after several scans of its region shown as an insert in Fig. 1b.

Since sodium already exists at the surface of the support, coating with PANI yielded a substantial attenuation of its Na Auger peak centred at an apparent binding energy of 496 eV. It is important to note that the casting solvent, HFIP, has been completely removed as there was no evidence of an F1s peak. HFIP is actually known to remain sorbed in some solvent-cast polymer coatings such as poly(acrylonitrile), nylon-6,6 and nylon-6 [29].

XPS surface composition analysis revealed that the carbon content of PANI coated on Chromosorb W is 40.1% which is more than two times larger than that of the uncoated support. C/N atomic ratio is much larger than 6 mainly due to the carbon content of the dopant. Using the S/N ratio, the dopant level was determined as 66% for PANI-HEBSA.

From the Si2p peak attenuation, the average

thickness of PANI at the surface of the support can be determined using the following equation:

$$I_{\text{Si2p}} = I_{\text{Si2p}}^0 \exp(-d/\lambda_{\text{Si2p}} \cos \theta) \quad (9)$$

where  $I_{\text{Si2p}}^0$  is the Si2p peak intensity obtained with the uncoated support,  $\lambda_{\text{Si2p}}$  is the mean free path of Si2p in the PANI adlayer,  $d$  is the PANI thickness, and  $\theta$  is the analysis take-off angle relative to the surface normal;  $\cos \theta$  can take the average value of 0.5 if we assume spherical powder particles [30].

$\lambda_{\text{Si2p}}$  is estimated using the Dench and Seah equations established for organics [31]:

$$\lambda = 0.11(E_{\text{K}})^{0.5} \text{ in mg/m}^2 \quad (10)$$

where  $E_{\text{K}}$  is the kinetic energy of the emitted Si2p core-electron. Assuming a density of 1.5 for PANI,  $\lambda_{\text{Si2p}} = 2.73 \text{ nm}$ .

Numerical application of Eq. (10) gives an average thickness of 2.6 nm for the PANI deposit considering the chromosorb particles as spherical. These values assume a continuous adlayer of PANI with a full coverage of the chromosorb.

### 4.2. Retention diagrams

Fourteen solutes were injected into two separate chromatographic columns containing PANI-EB and PANI-HEBSA. These solutes were selected to represent three chemically different families: alkanes, acetates, and alcohols. Each family was selected with a series of solutes with an increasing number of carbons in the solutes' backbone. Thus, alkanes will reveal the effect of the dispersive forces on the solubility of alkanes with PANI-EB and PANI-HEBSA and on the dispersive surface energy of both polymers. Acetates and alcohols will reveal the effect of dipole–dipole and H-bonding of solutes with the polymer backbone. From chromatographic retention times of solutes, the specific retention volumes  $V_{\text{g}}^{\circ}$  of all solutes were calculated according to Eq. (1). From  $V_{\text{g}}^{\circ}$  values, retention diagrams for all solutes were generated by plotting  $\ln V_{\text{g}}^{\circ}$  versus  $1/T$ .  $V_{\text{g}}^{\circ}$  values are described in Table 1 for PANI-EB in the temperature range of 140–170 °C and Table 2 for PANI-HEBSA (80–130 °C). Since PANI-EB and PANI-HEBSA have a high melting point, these temperature ranges were selected to ensure that both

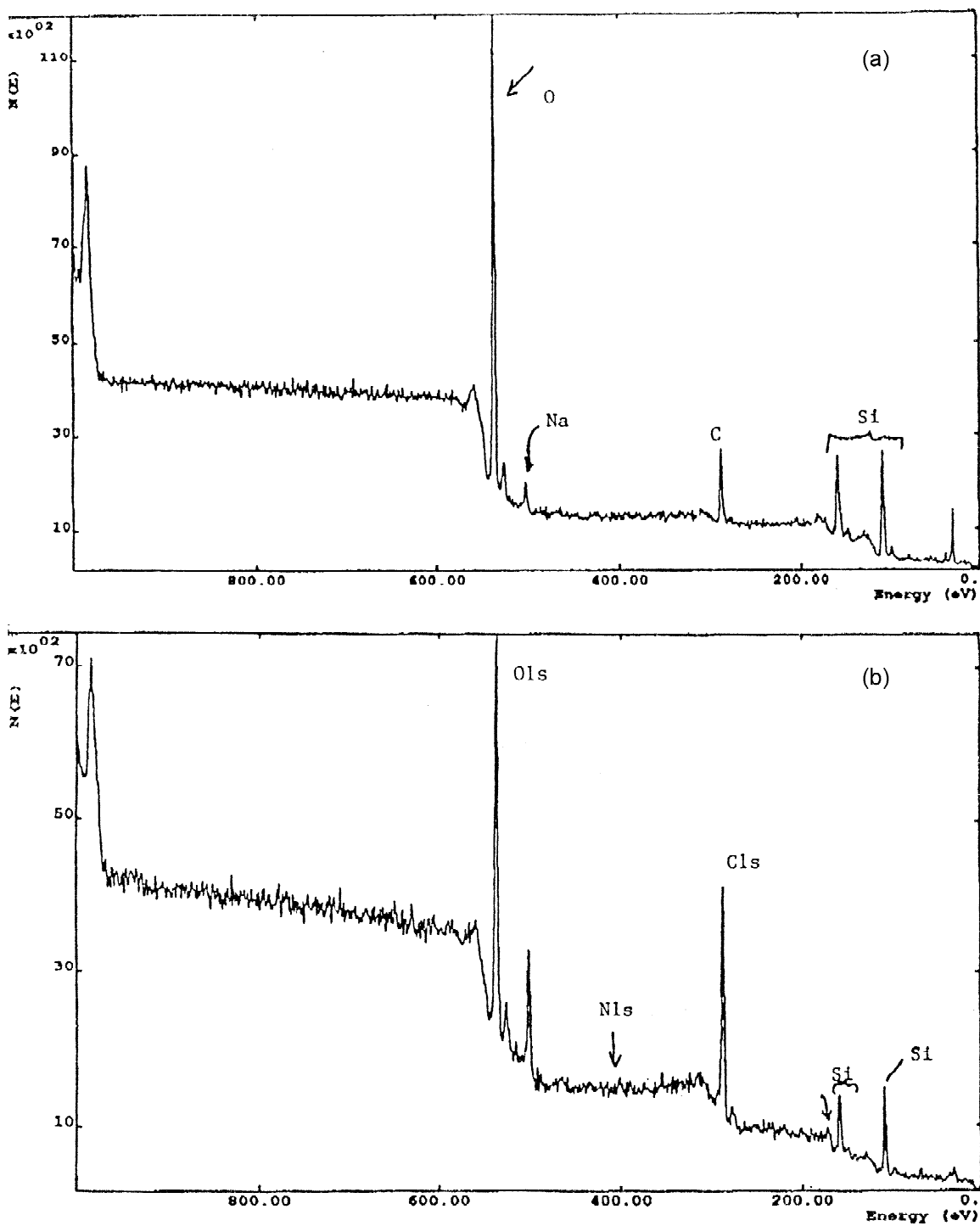


Fig. 1. (a) XPS survey scans of Chromosorb W. (b) XPS survey scans of PANI-HEBSA coated on Chromosorb W.

Table 1  
Specific retention volumes of solutes at a temperature range 140–170 °C for 7% PANI-EB

Solutes	140 °C	150 °C	160 °C	170 °C
Heptane	6.06	3.88	5.08	2.64
Octane	7.67	4.86	6.35	3.90
Nonane	10.41	7.25	6.68	4.89
Decane	16.59	7.74	10.39	6.95
Undecane	29.54	13.17	12.10	8.12
Dodecane	9.45	16.21	20.30	14.79
Methyl acetate	11.82	19.86	8.28	6.68
Ethyl acetate	13.42	23.39	10.08	9.29
Propyl acetate	15.36	27.38	10.58	13.38
Butyl acetate	7.20	29.34	13.36	16.03
Methanol	7.46	20.30	8.87	5.70
Ethanol	9.10	24.18	15.03	9.84
Propanol	6.99	26.13	10.56	8.68
Butanol	2.75	21.67	9.25	7.22

polymers are at temperatures higher than their glass transition temperatures, thus avoiding the kinetic effect on  $V_g^o$  values. It is evident from Tables 1 and 2 that all solutes interacted strongly with the conducting form PANI-HEBSA. It is of interest to mention that among the alkanes, undecane and dodecane showed stronger attraction than the rest of the alkanes due to the increase of the dispersive forces. On the other hand, methanol and ethanol showed stronger H-bonding with the conducting form than propanol and butanol (showed curvature at higher

Table 3  
Interaction parameters of alkanes at a temperature range 140–170 °C for 7% PANI-EB

Solutes	140 °C	150 °C	160 °C	170 °C
Heptane	0.48	0.67	0.14	0.55
Octane	0.89	1.07	0.54	0.55
Nonane	1.21	1.28	1.07	1.11
Decane	1.34	1.78	1.18	1.29
Undecane	1.36	1.82	1.58	1.67
Dodecane	3.07	2.15	1.59	1.58

temperatures), while this effect was not very clear in the case of the nonconducting form.

To ensure that the thermodynamics is valid in these ranges of temperature, a linear relationship of  $\ln V_g^o$  vs.  $1/T$  is an indication of the establishment of equilibrium between the mobile gaseous phase and the stationary phase. Figs. 2–4 show this relationship for alkanes, acetates, and alcohols with PANI-EB and Figs. 5–7 with PANI-HEBSA. A straight line was obtained in the case of alkanes–PANI-EB; however, a curvature was observed for acetates and alcohols with a maximum of around 145 °C. Such a curvature is an indication of a phase change from a semicrystalline to amorphous phase. Above 145 °C, PANI-EB is completely amorphous because experiments were performed at temperatures 50 °C above  $T_g$  to ensure the establishment of equilibrium. It is probable that both adsorption and absorption of

Table 2  
Specific retention volumes of solutes at a temperature range 80–130 °C for 7% PANI-HEBSA

Solutes	80 °C	90 °C	100 °C	110 °C	120 °C	130 °C
Pentane	14.75	14.10	15.14	13.99	13.32	12.41
Hexane	20.712	18.40	17.49	16.65	15.03	13.26
Heptane	27.83	22.63	19.61	20.42	17.00	16.39
Octane	40.78	36.00	33.88	27.55	18.74	20.48
Nonane	113.18	70.31	55.42	38.69	30.66	31.87
Decane	217.73	137.87	83.92	64.59	49.85	43.19
Undecane	–	267.22	174.17	128.44	80.25	62.875
Dodecane	–	–	337.06	223.24	138.93	114.661
Methyl acetate	39.99	22.45	22.63	23.86	20.16	19.53
Ethyl acetate	36.99	27.54	22.33	19.83	17.77	16.31
Propyl acetate	43.51	36.56	29.07	21.56	22.35	18.71
Butyl acetate	55.26	55.29	46.69	30.45	30.18	27.26
Methanol	463.33	295.52	217.46	161.27	139.89	114.40
Ethanol	415.31	254.85	199.11	176.27	146.48	130.44
Propanol	54.53	41.96	31.23	30.29	32.56	34.51
Butanol	59.27	43.77	34.32	35.66	29.87	33.65

Table 4

Interaction parameters of alkanes at a temperature range 80–130 °C for 7% PANI-HEBSA

Solute	80 °C	90 °C	100 °C	110 °C	120 °C	130 °C
Pentane	−0.35	−0.58	−0.93	−1.12	−1.33	−1.51
Hexane	0.20	0.01	−0.24	−0.48	−0.65	−0.79
Heptane	0.74	0.61	0.42	0.07	−0.04	−0.28
Octane	1.17	0.92	0.62	0.49	0.56	0.16
Nonane	0.95	1.01	0.86	0.85	0.74	0.37
Decane	1.09	1.08	1.16	1.02	0.89	0.69
Undecane	–	1.17	1.14	1.00	1.07	0.93
Dodecane	–	–	1.18	1.12	1.15	0.93

solutes with the polymer layer coexists provided that porosity exists in the polymer layer coated on the chromosorb support. Alkanes did not show such an indication of a phase change due to their weak interactions with PANI-EB as compared to the acetates and alcohols. As expected,  $V_g^o$  values increased as the number of carbons increased in the alkane series and decreased as the temperature increases.

It is noticeable from Figs. 2–4 that a strong scattering of data exists to a point that it was difficult to distinguish between the retention of solutes with

PANI-EB. This can be attributed to the instability of the PANI-EB surface which exhibits an abnormally weak density. Since IGC works with infinite dilution, this instability may be amplified because the infinite dilution conditions are sensitive to the sites having the highest energy that are also the most unstable and that it does not deliver any absolute data on a heterogeneous surface.

The linear relationship shown in Figs. 2–7 can yield the molar heat (enthalpy) of sorption of solutes absorbed by PANI-EB and PANI-HEBSA as a slope of the straight lines according to Eq. (4). Table 5

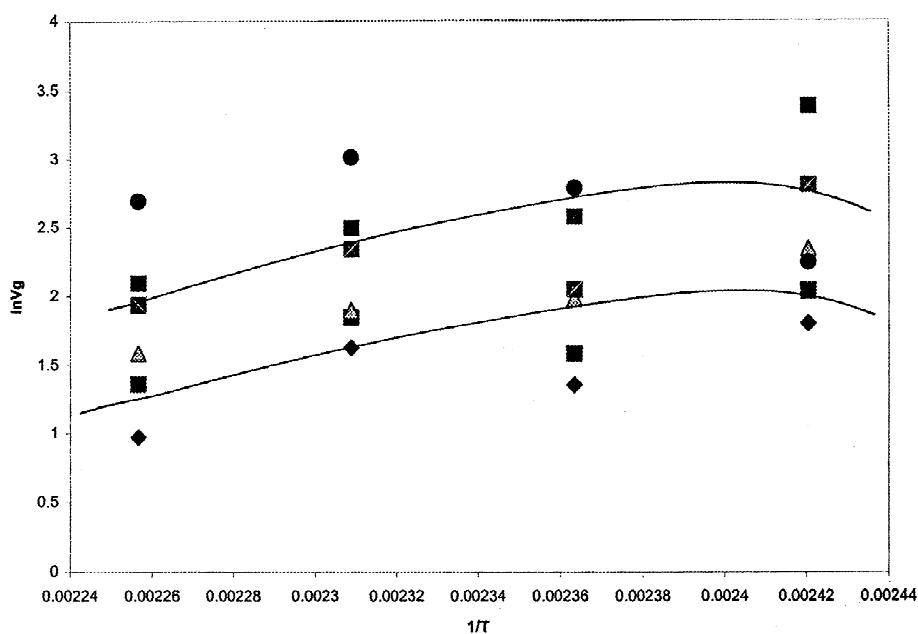


Fig. 2. Dependence of  $V_g$  of alkanes–PANI-EB on temperature (130–170 °C). ♦, Heptane; ■, octane; ▲, nonane; ■, decane; ■, undecane; ●, dodecane.



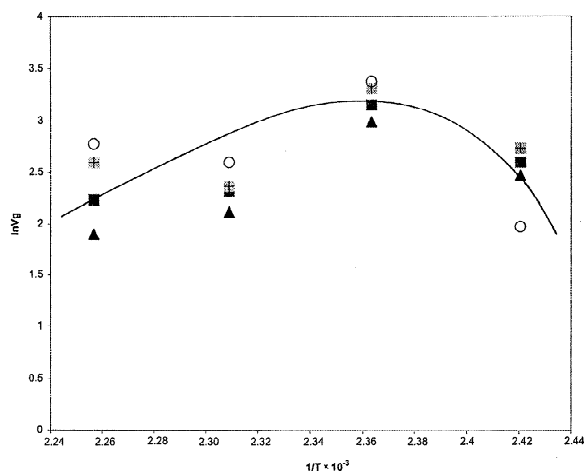


Fig. 3. Dependence of  $V_g$  of acetates–PANI-EB on temperature (130–170 °C). ▲, Methyl acetate; ■, ethyl acetate; ■, propyl acetate; ○, butyl acetate.

shows the exothermic molar heat of sorption of the three families for both PANI-EB and PANI-HEBSA. The sorption process involves the transfer of the solute molecules from the vapor phase into the amorphous part of the polymer. This process strongly depends on the polymer–solute interaction,  $\chi_{12}$ , and therefore the heat of sorption associated with this process depends on the interaction too. This effect can be seen clearly with doped PANI (PANI-HEBSA); the  $\Delta H_1^s$  value has increased considerably (–3.35 to –46.44 kJ/mol) while the  $\Delta H_1^s$  for the

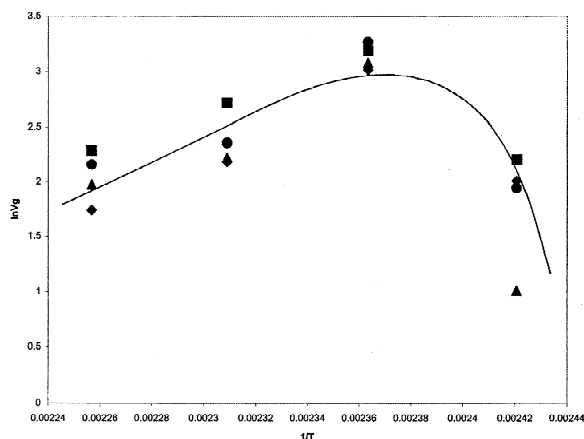


Fig. 4. Dependence of  $V_g$  of alcohols–PANI-EB on temperature (130–170 °C). ◆, Methanol; ■, ethanol; ●, propanol; ▲, butanol.

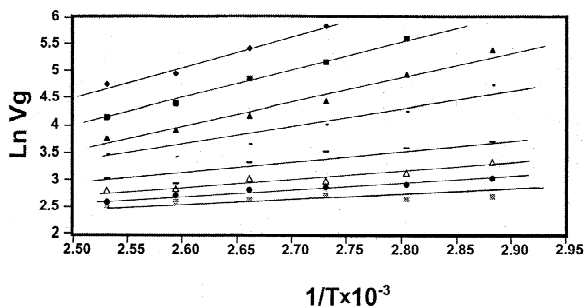


Fig. 5. Dependence of  $V_g$  of alkanes–PANI-HEBSA on temperature (80–130 °C). ■, Pentane; ●, hexane; △, heptane; -, octane; •, nonane; ▲, decane; ■, undecane; ◆, dodecane.

undoped PANI (PANI-EB) averaged about –0.03 kJ/mol. The observed big difference in  $\Delta H_1^s$  values between both polymers reflects the surface properties of both polymers, clearly showing the effect of the charged surface of PANI-HEBSA on solute interactions.

For the PANI-HEBSA, increasing the number of  $\text{CH}_2$  groups in alkanes has increased the exothermic molar heat of sorption and higher alkanes showed a significant increase of solubility than the lower alkanes. The increase of  $\text{CH}_2$  group in the acetate family did not show a marked effect on the molar heat of sorption due to the chain being considerably shorter than alkanes. The molar heat of sorption of acetates and alcohols ranged about –0.08 kJ/mol for PANI-EBA and is due to pure dipole–dipole and

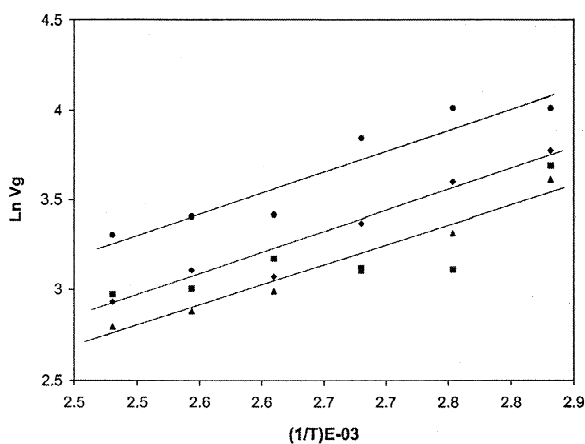


Fig. 6. Dependence of  $V_g$  of acetates–PANI-HEBSA on temperature (80–130 °C). ■, Methyl acetates; ▲, ethyl acetates; ◆, propyl acetates; ●, butyl acetates.

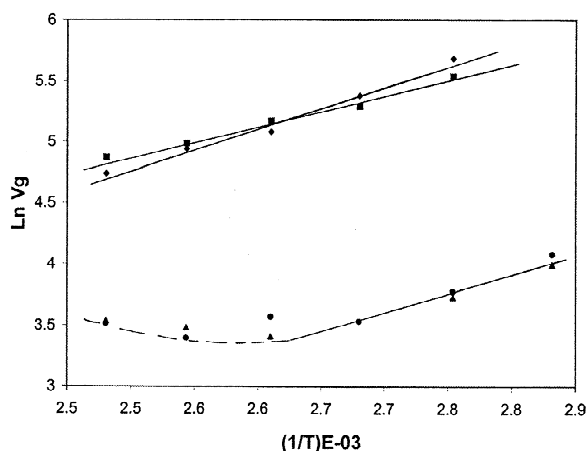


Fig. 7. Dependence of  $V_g$  of alcohols–PANI-HEBSA on temperature (80–130 °C).  $\blacklozenge$ , Methanol;  $\blacksquare$ , ethanol;  $\blacktriangle$ , propanol;  $\bullet$ , butanol.

H-bonding interactions. There was no distinction between acetates and alcohols interactions; all behaved the same. This is not the case when the polymer is conductive; PANI-EBA showed a distinctive trend of dependency when acetates and alcohols are used. In particular, methyl and ethyl alcohols showed the strongest interactions among the group. This exothermicity shows the effect of the combination of dispersive with the hydrogen bonding attraction forces.

#### 4.3. Thermodynamic parameters

The PANI-EB– and PANI-HEBSA–solute interaction parameters were calculated according to Eq. (2) for all solutes and in the temperature range 140–170 °C. At this temperature range, the polymer is at melt and therefore, an equilibrium is established and the thermodynamics becomes valid. Table 3 shows the PANI-EB–alkanes interaction parameters which ranged from +0.40 for heptane to +1.50 for dodecane. The endothermic nature of these data indicate the poor interaction of alkanes with PANI-EB as expected. However, the interaction parameters did show a considerable variation with increasing number of carbons in the alkane family. However, PANI-HEBSA showed an opposite behavior due to the polar surface. The interaction parameters ranged from –1.50 to +1.2 showing the exothermic nature of the solute interaction with the surface (Table 4). It is clear that the temperature had a marked effect on the interaction parameters which decreased as the temperature increased and is characteristic of the strong interaction. It is also interesting to note that higher alkanes showed less interaction parameters than lower alkanes (Fig. 8).

Petri and Wolf [32] suggested that the temperature dependence of  $\chi$  at different concentrations demonstrates that the heat of dilution generally increases with increasing concentration; whereas, the noncom-

Table 5  
Molar heat of sorption,  $\Delta H_1^s$ , of both PANI-EB and PANI-HEBSA

Solutes	$\Delta H_1^s$ , PANI-EB (kJ/mol)	$\Delta H_1^s$ , PANI-HEBSA (kJ/mol)
Pentane	–0.04	–3.68
Hexane	–0.04	–9.71
Heptane	–0.04	–11.80
Octane	–0.04	–18.91
Nonane	–0.04	–31.34
Decane	–0.04	–38.79
Undecane	–0.04	–44.64
Dodecane	–0.04	–46.36
Methyl acetate	–0.08	–13.31
Ethyl acetate	–0.08	–18.87
Propyl acetate	–0.08	–20.38
Butyl acetate	–0.08	–19.54
Methanol	–0.08	–32.47
Ethanol	–0.08	–25.86
Propanol	–0.08	–10.75
Butanol	–0.08	–13.60

Table 6  
Dispersive surface energies of PANI-EB and PANI-HEBSA and  $\gamma_{\text{CH}_2}$

Temperature (°C)	PANI-EB surface energy, $\gamma_s^d$ (mJ/m <sup>2</sup> )	PANI-HEBSA surface energy $\gamma_s^d$ (mJ/m <sup>2</sup> )	CH <sub>2</sub> surface energy $\gamma_{\text{CH}_2}$ (mJ/m <sup>2</sup> )
80	–	150.24	32.16
90	–	137.81	31.58
100	–	100.31	31.00
110	–	100.95	30.42
120	–	78.96	29.84
130	–	74.27	29.26
140	29.13	–	28.68
150	71.77	–	28.10
160	63.63	–	27.52
170	94.05	–	26.94

binatorial entropy of dilution decreases. This may lead to a linear interdependence of the enthalpy and entropy part of  $\chi$ . Accordingly, plots of  $\chi$  vs. the inverse of temperature for 7% load of PANI-EB and PANI-HEBSA were made according to the following equations:

$$\chi_H = \frac{\Delta H_1}{RT\phi_2^2} = \frac{1}{T} \cdot \left( \frac{\delta\chi}{\delta(1/T)} \right) \quad (11)$$

and

$$\chi_S = \chi \cdot \chi_H = \frac{\Delta S_1^R}{R\phi_2^2} \quad (12)$$

where  $\chi_H$  and  $\chi_S$  are the enthalpy and entropy contributions to the interaction parameters.  $\Delta H_1$  is the molar heat of dilution,  $\Delta S_1^R$  is the entropy of dilution and  $\phi_2$  is the volume fraction of PANI. Fig. 9 shows the temperature dependence of  $\chi$  of PANI-EB. A similar plot for PANI-HEBSA yielded an intercept of 0.90 kJ/mol as the contribution of entropy of dilution to the interaction parameters, and a slope of 2.91 kJ/mol. Fig. 9 is a plot for the nonconducting form PANI-EB and showed an intercept of 0.7 kJ/mol and a slope of 0.699 kJ/mol, characteristics of the inert nature of the surface.

#### 4.4. Surface energy

In order to evaluate the dispersive component of the surface energy of both PANI-EB (non-conducting) and PANI-HEBSA (conducting), plots of  $(RT \ln V_g^0)$  versus the number of carbons in the alkane series were generated for each temperature using Eq. (7) (Figs. 10 and 11). A linear relationship was obtained in all of these plots and the slopes of the straight lines were computed as the free energy of desorption of a CH<sub>2</sub> group,  $\Delta G_a^{\text{CH}_2}$ . Utilizing Eq. (11), the dispersive component of the surface energy of these two polymers was calculated as a function of temperature. The cross-sectional area of an adsorbed CH<sub>2</sub> group,  $a_{\text{CH}_2}$  is estimated to be 6 Å<sup>2</sup> [33,34]. The surface-free energy of a solid containing only CH<sub>2</sub> groups,  $\gamma_{\text{CH}_2}$ , is computed as a function of temperature as follows:

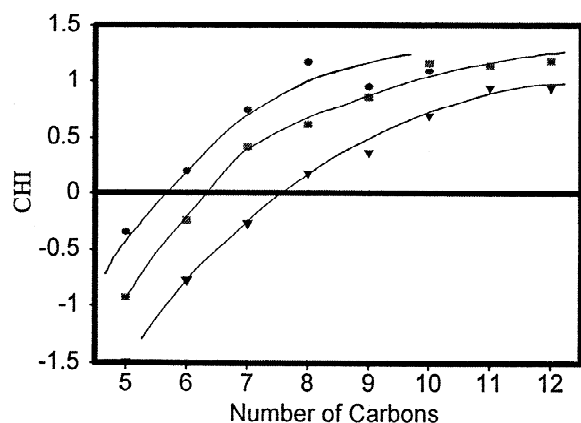


Fig. 8. The dependence of the interaction parameter,  $\chi_{12}$  of PANI-EB on number of carbons in the alkane series. ▼, 80 °C; ■, 100 °C; ●, 130 °C.

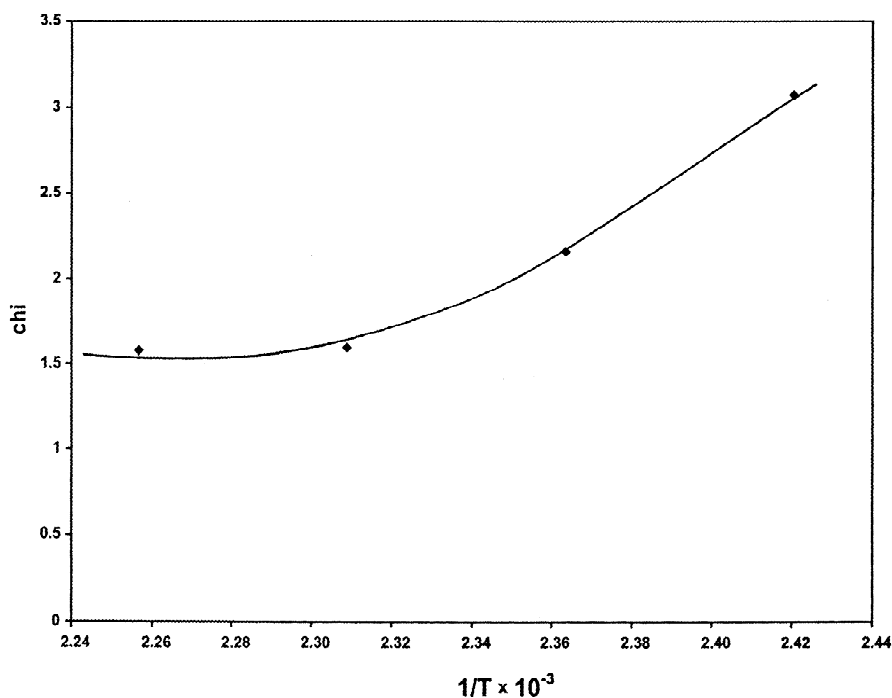


Fig. 9. The temperature dependence of the interaction parameter,  $\chi_{12}$  of PANI-EB–dodecane.  $\blacklozenge$ , Dodecane.

$$\gamma_{\text{CH}_2} = 36.80 - 0.058T \quad (13)$$

where  $T$  is the temperature in  $^{\circ}\text{C}$ . Recently, we measured the dispersive component of the surface

energy of PVMK (poly(vinyl methyl ketone)) [21], PEO (polyethylene oxide) [20] and  $\text{PVF}_2$  (poly(vinylidene fluoride)) blends [35] in a similar way.

Table 6 shows the dispersive surface energy of both non-conducting and conducting polyaniline as a

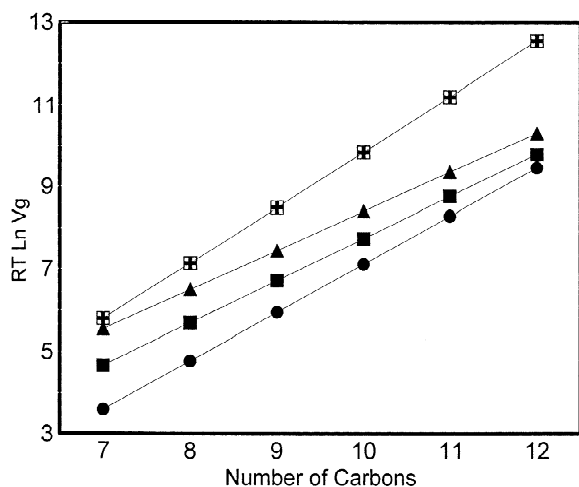


Fig. 10.  $RT \ln V_g$  dependence on number of carbons in the alkane family, PANI-EB.  $\blacksquare$ , 130  $^{\circ}\text{C}$ ;  $\square$ , 140  $^{\circ}\text{C}$ ;  $\blacktriangle$ , 150  $^{\circ}\text{C}$ ;  $\bullet$ , 170  $^{\circ}\text{C}$ .

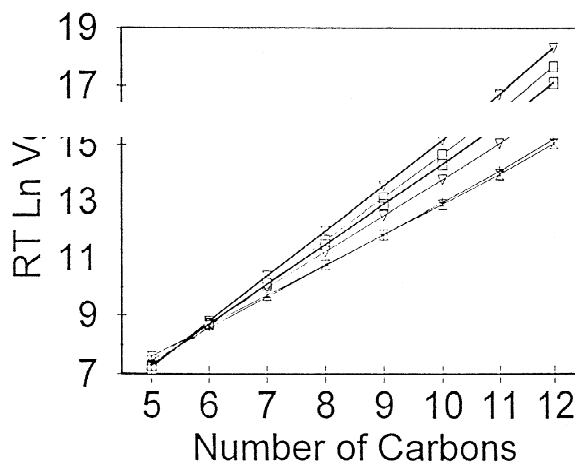


Fig. 11.  $RT \ln V_g$  dependence on number of carbons in the alkane family, PANI-HEBSA.  $\square$ , 80  $^{\circ}\text{C}$ ;  $\blacksquare$ , 90  $^{\circ}\text{C}$ ;  $\nabla$ , 100  $^{\circ}\text{C}$ ;  $\blacktriangledown$ , 110  $^{\circ}\text{C}$ ;  $+$ , 120  $^{\circ}\text{C}$ ;  $\times$ , 130  $^{\circ}\text{C}$ .

function of temperature. The dispersive surface energy of the non-conducting PANI-EB ranged from 29.13 mJ/m<sup>2</sup> at 140 °C to 94.05 mJ/m<sup>2</sup> at 170 °C, while the surface energy of the conducting PANI-HEBSA showed higher values (150.24 mJ/m<sup>2</sup> at 80 °C to 74.27 mJ/m<sup>2</sup> at 130 °C).  $\gamma_s^d$  values for PANI-EB showed reasonable values at 140 °C as compared to other polymers (Table 7); however, at higher temperatures, the values are higher than expected. The trend of the  $\gamma_s^d$  change direction is also surprising and unexpected. Further examination of the data reveals that as the polymer is heated from 140 to 170 °C, the surface of the polymer was activated and perhaps created some nano-pores resulting in an increase in surface energy of the non-conducting form.

The surface energy of the conducting form showed an expected trend of decreasing as the temperature increased. Similar results were found with PpyCl; the surface energy was decreased after the column was thermally treated [15]. XPS analysis of the thermally treated column revealed a decrease in doping level and an increase in the C–N imine defects. This is in agreement with earlier results reported by Schmitt et

al. [36], who observed a decrease of the surface energy of treated CaCO<sub>3</sub> with increasing temperature. At these temperatures, the surface of these polymers expands. Thus, the surface energy decreases and allows the vapor to penetrate the surface. Similar observations were reported on a heat-treated SiO<sub>2</sub> Xerogel [19]. The  $\gamma_s^d$  values varied from 49.07 mJ/m<sup>2</sup> at 25 °C to 17.20 mJ/m<sup>2</sup> at 150 °C.

$\gamma_s^d$  values for PANI-HEBSA showed surprisingly higher than anticipated values of its class (Table 7). Our data indicate that PANI-HEBSA doped with ethylbenzenesulfonic acid is a high energy material. There are conflicting reports in the literature regarding  $\gamma_s^d$  values [19,37,38].  $\gamma_s^d$  values measured by IGC [24] on PANI and PANI-silica showed values ranging between 87.3 and 130.00 mJ/m<sup>2</sup> at a temperature range of 60 to 80 °C. However,  $\gamma_s^d$  values obtained on PANI by methods other than IGC such as wettability measurements [37] and geometric mean method [38] showed lower values than IGC (42.60 mJ/m<sup>2</sup>). In a recent report, Vickers et al. [34] reported the  $\gamma_s^d$  values of PAN-based carbon fibers which ranged from 104 mJ/m<sup>2</sup> for untreated fibers at 50 °C to 78 mJ/m<sup>2</sup> for 200% oxidized fibers.

Table 7  
Comparative data on  $\gamma_s^d$  in mJ/m<sup>2</sup> of several polymers, blend and mercury

Polymer	$\gamma_s^d$ (mJ/m <sup>2</sup> )	Temperature (°C)	Ref.
Undoped PANI	29.00–94.00	140–170	This work
Doped PANI	74.00–150.00	80–130	This Work
PANI	87.3	68	[24]
PANI-Silica	130	60–80	[24]
PANI <sup>a</sup>	42.6	58	[37]
PANI <sup>b</sup>	42.6	58	[38]
PVF <sub>2</sub> –PVMK blend	36.24	82	[35]
PEO	11.04	77	[20]
PVMK	26.47	77	[21]
Hg	200.00	20	[26]
PVC	41.50	20	[38]
PMMA	40.00	20	[24]
Polypropylene	28.90		[33]
Polyurethane	20.30		[33]
Polyethylene	33.10		[33]
Cl-doped Ppy <sup>c</sup>	42.00		[15]
NO <sub>3</sub> <sup>-</sup> doped Ppy	61.20		[22]
Fe(CN) <sub>6</sub> <sup>4-</sup> doped Ppy	106.00		[22]
PTEF	19.00	20	[33]

<sup>a</sup> Derived from wettability measurements.

<sup>b</sup> Derived from geometric mean method.

<sup>c</sup> Ppy is polypyrrole.

It is evident from Table 6 that  $\gamma_s^d$  values for PANI-HEBSA decreased as the temperature increased due to the expansion of the surface and the microstructure reorganization. We are able to compare values for surface energy of both forms with other polymers measured by methods such as NMR and FTIR. Table 7 shows comparative data on the surface energies of several polymers relative to mercury. Comparing these data with the surface energy of conducting polymers [15,22] the surface energy of the non-conducting form at 140 °C is close to polypropylene, polyurethane, and polyethylene [33]; however, the  $\gamma_s^d$  values above 140 °C are not comparable to the non-conducting polymers.  $\gamma_s^d$  values of the conducting form are surprisingly high as compared to other conducting polymers. The dispersive component to the surface energy of several polypyrroles is in the range of 30–60 mJ/m<sup>2</sup>, while conducting polypyrroles have a much higher surface energy, 106 mJ/m<sup>2</sup> [15,22]. Based on the dispersive properties, polypyrroles and PANI are considered to be conductive polymers unlike the conventional insulating forms and their surface energies are comparable to those of graphite, metal oxides, and surface-modified carbon fibers.

## Acknowledgements

The authors wish to acknowledge Dr. Mohammed M. Chehimi of ITDOS, Universite de Paris for fruitful discussion regarding the surface analysis and the surface energy results of PANI. We are also grateful to Ms. Carole Connan of the same institution for her technical assistance with XPS measurements.

## References

- [1] Y. Cao, P. Smith, A. Heeger, J. Synth. Metals 48 (1992) 91.
- [2] Z.Y. Al-Saigh, Int. J. Polymer Anal. Characterization 3 (1997) 249.
- [3] Z.Y. Al-Saigh, P. Chen, Macromolecules 24 (1991) 3788.
- [4] J. Guillet, Z.Y. Al-Saigh, Inverse gas chromatography in analysis of polymers and rubbers, in: R. Meyers (Ed.), Encyclopedia of Analytical Chemistry: Instrumentation and Applications, Vol. 9, Wiley, Chichester, 2000, p. 7759.
- [5] H. Balard, E. Papirer, Progr. Org. Coat. 22 (1993) 1.
- [6] E. Papirer, J. Schultz, C. Turchi, Eur. Polymer J. 20 (1984) 1155.
- [7] E. Papirer, J. Schultz, J. Jagiello, R. Baeza, R.F. Clauss, H.A. Mottola, J.R. Steinmetz (Eds.), Chemically Modified Surfaces, Elsevier, Amsterdam, 1992, p. 334.
- [8] J. Kuczinski, E. Papirer, Eur. Polym. J. 27 (1991) 653.
- [9] E. Papirer, P. Roland, M. Nardin, H. Balard, J. Colloid Interface Sci. 113 (1986) 62.
- [10] E. Papirer, H. Balard, A. Vidal, Eur. Polym. J. 24 (1988) 783.
- [11] G. Ligner, A. Vidal, H. Balard, E. Papirer, J. Colloid Interface Sci. 133 (1989) 200.
- [12] C. Filbert, Diplome d'Etudes Approfondies, Universite de Haute Alsace, Mulhouse, 1989.
- [13] E. Papirer, G. Ligner, A. Vidal, H. Balard, H.F. Mauss, in: E. Leyden, W.T. Collins (Eds.), Chemically Modified Oxide Surfaces, Gordon and Breach, New York, 1990, p. 361.
- [14] E. Papirer, A. Eckhardt, F. Muller, J. Yvon, J. Mater. Sci. 25 (1990) 5109.
- [15] M.M. Chehimi, M.-L. Abel, E. Pigois-Landureau, M. Delamar, Synth. Metals 60 (1993) 183.
- [16] P. Schmitt, E. Koerper, J. Schultz, E. Papirer, Chromatographia 25 (1988) 786.
- [17] C. Saint Flour, E. Papirer, J. Colloid Interface Sci. 91 (1983) 69.
- [18] F. Chen, Macromolecules 21 (1988) 1640.
- [19] F. Rubio, J. Rubio, J.L. Oteo, J. Sol-Gel Sci. Technol. 18 (2000) 115.
- [20] Z.Y. Al-Saigh, Polymer 40 (1999) 3479.
- [21] Z.Y. Al-Saigh, Polymer Int. 40 (1996) 25.
- [22] M.M. Chehimi, E. Pigois-Landureau, M.M. Delamar, J. Chim. Phys. 89 (1992) 1173.
- [23] E. Landureau, M.M. Chehimi, J. Appl. Polym. Sci. 49 (1993) 183.
- [24] M.M. Chehimi, M.L. Abel, C. Perruchot, M. Delamar, S.F. Lascelles, S.P. Armes, Synth. Metals 104 (1999) 51.
- [25] F.M. Fowkes, Ind. Eng. Chem. Prod. Res. Dev. 56 (1967) 40.
- [26] F.M. Fowkes, Ind. Eng. Chem. 561 (1964) 40.
- [27] Z.Y. Al-Saigh, P. Munk, Macromolecules 17 (1984) 803.
- [28] T.W. Card, Z.Y. Al-Saigh, P. Munk, J. Chromatogr. 301 (1984) 261.
- [29] G. Beamson, D. Briggs, High Resolution XPS of Organic Polymers—The Scienta ESCA300 Database, Wiley, Chichester, 1992, pp. 184–185, 196–199.
- [30] T.J. Carney, P. Tsakiroopoulos, J.F. Watts, J.E. Castle, Int. J. Rapid Solidification 5 (1990) 189.
- [31] D. Briggs, M.P. Seah (Eds.), Auger and X-Ray Photoelectron Spectroscopy, 2nd ed, Practical Surface Analysis, Vol. 1, Wiley, Chichester, 1990, p. 209.
- [32] H.M. Petri, B.A. Wolf, Macromolecules 27 (1994) 2714.
- [33] C. Bonnerup, P. Gatenholm, J. Adhes. Sci. Technol. 7 (1993) 247.
- [34] P.E. Vickers, J.F. Watts, C. Perruchot, M.M. Chehimi, Carbon 38 (2000) 675.

- [35] A. Al-Gahmdi, Z.Y. Al-Saigh, *J. Polymer Sci. Part B: Polymer Phys.* B38 (2000) 1155.
- [36] P. Schmitt, E. Koerper, J. Schultz, E. Papirer, *Chromatographia* 25 (1988) 786.
- [37] B. Wessling, in: 2nd ed, *Handbook of Conducting Polymers*, Marcel Dekker, New York, 1998.
- [38] S. Wu, *Polymer Interface and Adhesion*, Marcel Dekker, New York, 1982.